

Engineered Multilayer Colloidal Crystals with Tunable Optical Properties

Pascal Massé and Serge Ravaine*

Centre de Recherche Paul Pascal - CNRS, 115, avenue du Dr Schweitzer - 33600 Pessac, France

Received March 17, 2005. Revised Manuscript Received May 26, 2005

Multilayer colloidal crystals with a perfectly defined architecture have been fabricated by the successive depositions of layers of silica particles with various diameters onto a substrate. The composite materials have been characterized by scanning electron microscopy (SEM) and near-infrared (NIR) spectroscopy. Our results establish that the optical properties of these multilayer systems can be tailored by adjusting either the thickness or the stacking order of each component crystal. The versatility of our approach has been further exploited to fabricate a multilayer colloidal crystal consisting of many alternating layers of two different spheres sizes.

Introduction

In recent years, there has been tremendous activity in an attempt to fabricate and investigate the structure–property relationship of three-dimensional (3D) photonic crystals.¹ A key property of these materials is the presence of a photonic band gap, analogous to electronic band gap in a semiconductor, which arises from the inhibition of the electromagnetic waves propagation over a certain range of frequency. Thus, photonic crystals are promising tools to manipulate, confine, and control light, and they have been proposed for applications such as optical filters,² switches,³ chemical and biological sensors,^{4,5} or waveguides for optoelectronics.⁶ As they can be readily assembled into long-range-ordered lattices, monodisperse colloidal particles are suitable building blocks for the elaboration of such materials. Several methods have been developed to organize colloids in such periodic arrays with well-defined crystal structures, sufficient domain sizes, and well-controlled thickness. Among those are sedimentation,⁷ electrophoretic deposition,⁸ physical confinement,⁹ multilayer deposition using the Langmuir–Blodgett technique,^{10,11} and vertical deposition.^{12,13} Nevertheless, the

formation of 3D lattices with arbitrary structures, which should exhibit interesting optical or nonlinear optical functionality, has met with limited success by using all of these procedures. Colvin and co-workers have first reported the fabrication of multilayer colloidal crystals consisting of successively stacked crystals, formed of colloids of arbitrary diameters.^{14,15} These new samples may afford opportunities for engineered photonic behavior. More recently, Ozin and co-workers have reported the fabrication of high-quality similar structures by the isothermal heating evaporation-induced self-assembly technique.¹⁶ Nevertheless, the optical behavior of these composite materials was not mentioned. Herein, we report the fabrication by the Langmuir–Blodgett technique of multilayer crystals with a perfect control of the thickness of each of their component stacks. We investigate the structure–optical properties relationship of these materials. Our results demonstrate that their optical behavior can be tailored by manipulating the thickness and the stacking order of each component crystal. By the successive depositions of alternating layers of two different sphere sizes, we are able to build a multilayer system with an original architecture and complex optical properties.

Experimental Section

Materials. Tetraethoxysilane (TEOS, Fluka), ammonia (29% in water, J. T. Baker), and (aminopropyl)triethoxysilane (Aldrich) were purchased in their reagent grade and were used without further purification. Deionized water was obtained with a MilliQ system (Millipore) whereas ethanol (EtOH) and chloroform (CHCl₃) were purchased from Prolabo.

Methods. 385- and 590-nm silica particles were synthesized following the well-known Stöber–Fink–Bohn method.¹⁷ Their

* Author to whom correspondence should be addressed. Tel: (33)556845667. Fax: (33)556845600. E-mail: ravaine@crpp-bordeaux.cnrs.fr.

- (1) Joannopoulos, J. D.; Meade, R. D.; Winn, J. N. *Photonic Crystals: Molding the Flow of Light*, 1st ed.; Princeton University Press: Princeton, NJ, 1995.
- (2) Park, S. H.; Xia, Y. *Langmuir* **1999**, *15*, 266.
- (3) Pan, G.; Kesavamoorthy, R.; Asher, S. A. *Phys. Rev. Lett.* **1997**, *78*, 3860.
- (4) Holtz, J.; Asher, S. A. *Nature* **1997**, *389*, 829.
- (5) Nelson, R.; Haus, J. W. *Appl. Phys. Lett.* **2003**, *83*, 1089.
- (6) Lin, S. Y.; Chow, E.; Hietala, V.; Villeneuve, P. R.; Joannopoulos, J. D. *Science* **1998**, *282*, 274.
- (7) Garcia-Santamaria, F.; Salgueirino-Maceira, V.; Lopez, C.; Liz-Marzan, L. M. *Langmuir* **2002**, *18*, 4519.
- (8) Holgado, M.; Garcia-Santamaria, F.; Blanco, A.; Ibisate, M.; Cintas, A.; Miguez, H.; Serna, J. C.; Molpeceres, C.; Requena, J.; Mifsud, A.; Meseguer, F.; Lopez, C. *Langmuir* **1999**, *15*, 4701.
- (9) Park, S. Y.; Qin, D.; Xia, Y. *Adv. Mater.* **1998**, *10*, 1028.
- (10) Reculosa, S.; Ravaine, S. *Chem. Mater.* **2003**, *15*, 598.
- (11) Szekeres, M.; Kamalin, O.; Schoonheydt, R. A.; Wostyn, K.; Clays, K.; Persoons, A.; Dékány, I. *J. Mater. Chem.* **2002**, *12*, 3268.
- (12) Jiang, P.; Bertone, J. F.; Hwang, K. S.; Colvin, V. L. *Chem. Mater.* **1999**, *11*, 2132.

- (13) Im, S. H.; Kim, M. H.; Park, O. O. *Chem. Mater.* **2003**, *15*, 1797.
- (14) Jiang, P.; Ostojic, G. N.; Narat, R.; Mittleman, D. M.; Colvin, V. L. *Adv. Mater.* **2001**, *13*, 389.
- (15) Rengarajan, R.; Jiang, P.; Larrabee, D. C.; Colvin, V. L.; Mittleman, D. M. *Phys. Rev. B* **2001**, *64*, 205103.
- (16) Wong, S.; Kitaev, V.; Ozin, G. A. *J. Am. Chem. Soc.* **2003**, *125*, 15589.
- (17) Stöber, W.; Fink, A.; Bohn, E. *J. Colloid Interface Sci.* **1968**, *26*, 62.

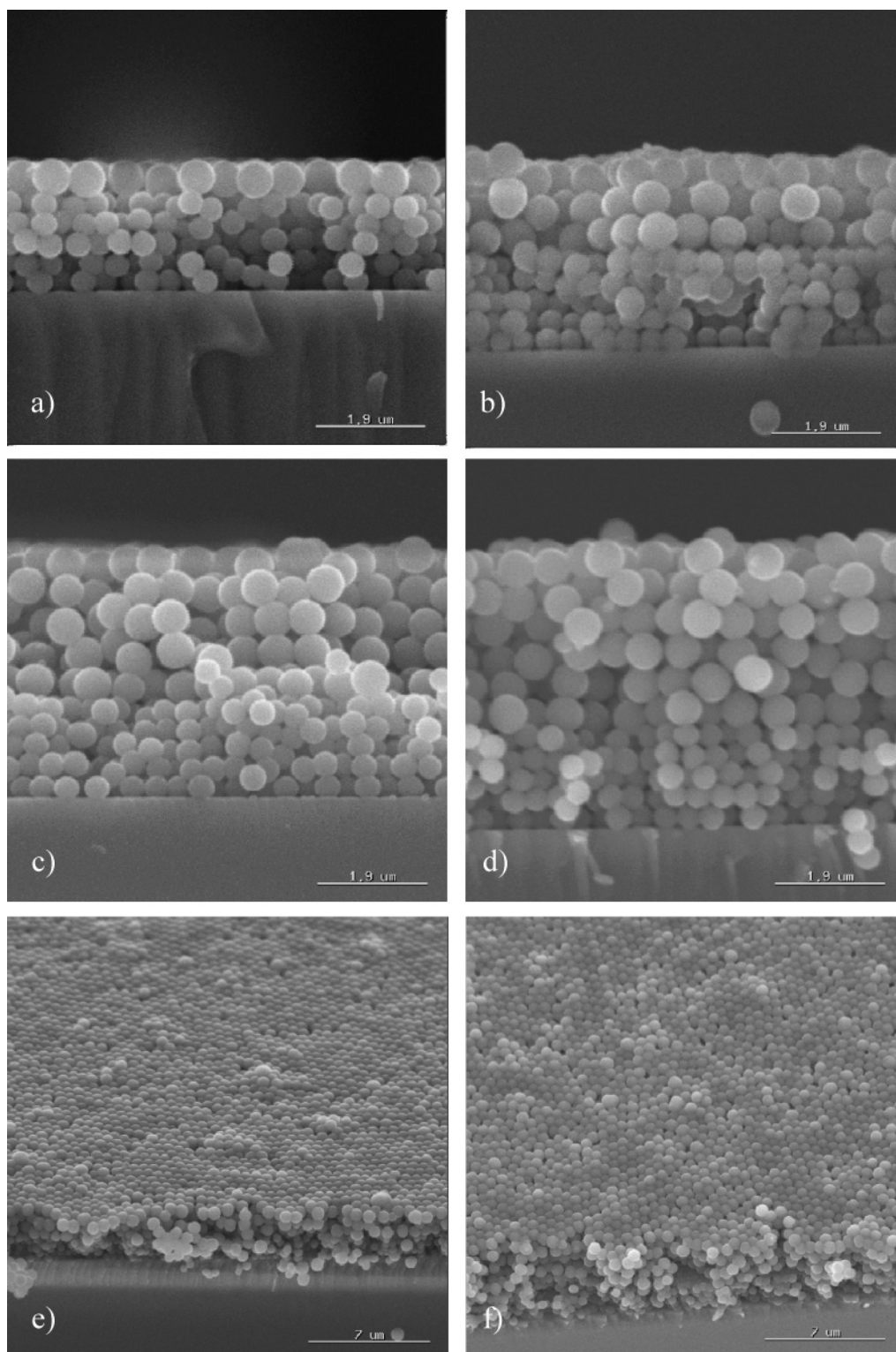


Figure 1. SEM side views of multilayer colloidal crystals made of one, three, five, and six (from a to d) layers of 590-nm silica particles on the top of five layers of 385-nm silica beads and SEM top views of $(385 \text{ nm})_5/(590 \text{ nm})_3$ (e) and $(385 \text{ nm})_5/(590 \text{ nm})_4$ (f) colloidal crystals.

functionalization with (aminopropyl)triethoxysilane was carried out as previously described.¹⁰

Multilayer colloidal crystals were fabricated by the Langmuir–Blodgett technique. Silica particles were first dispersed in an 80%/20% mixture of chloroform and ethanol. This suspension was sonicated for several minutes and was delicately spread out at the air–water interface in a Langmuir trough. Silica particles were compressed using a mobile barrier at room temperature (20 ± 1 °C) until a surface pressure of ca. $6 \text{ mN}\cdot\text{m}^{-1}$. A hydrophilic glass slide was then quickly immersed in the subphase (downstroke

speed: $10 \text{ cm}\cdot\text{min}^{-1}$) and was slowly pulled up out of the water (upstroke speed: $0.1 \text{ cm}\cdot\text{min}^{-1}$) so that a monolayer of particles was transferred onto the substrate only during the upstroke. Repeating this transfer process led to a crystalline three-dimensional array of particles with a controlled thickness, as the number of layers corresponded to the number of transfer cycles. This sample was immersed in another Langmuir trough, where a monolayer of silica spheres of different diameter had been formed as described above. Repeating the transfer process a precise number of times allowed us to elaborate colloidal crystals made of stacks of particles of

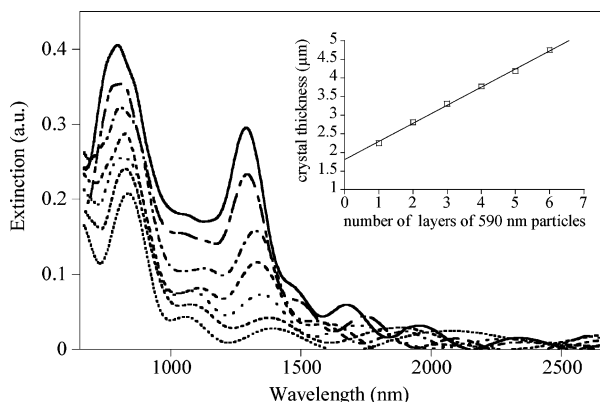


Figure 2. NIR transmission spectra of colloidal crystals made of zero to six (from bottom to top) layers of 590-nm silica particles on the top of five layers of 385-nm silica beads. The inset shows the evolution of the thickness of the composite materials (calculated from the positions of the Fabry–Pérot fringes) as a function of the number of layers of 590-nm silica particles.

different sizes. SEM observations were performed with a JEOL JSM-840A scanning electron microscope operating at 10 kV. The specimens were carbon-coated prior to examination. Near-infrared (NIR) spectra were recorded on a Magna-IR Spectrometer 750 from Nicolet.

Results

Figure 1 shows SEM side views of colloidal crystals composed by a varying number of layers of 590-nm silica particles deposited onto five layers of 385-nm silica beads. We describe the multilayer colloidal crystal pattern by listing the sphere size from bottom to top. For instance, the sample in Figure 1b is referred to as $(385 \text{ nm})_5/(590 \text{ nm})_3$. One can see that each component stack is a face-centered cubic (fcc) crystal film of silica spheres with (111) planes oriented parallel to the surface of the substrate. A closer look shows that larger silica particles assemble on layers of smaller ones just as they do on a flat surface, accordingly to previously reported results.^{14,15} The thickness of each stack is controlled at the layer level as the number of deposited layers matches perfectly with the predefined value of transfer cycles. The top surface of the multilayer crystals is smooth as shown on the SEM top views (Figure 1e and f), indicating the good crystalline quality of the overall structure. Figure 2 shows the NIR transmission spectra of the composite materials and of the crystal made of five layers of 385-nm silica particles. The latter one displays one intense peak around 830 nm, which arises from the Bragg diffraction of incident light (see bottom curve in Figure 2). At wavelengths higher than the stop-band position, Fabry–Pérot fringes are also observed. Such oscillations are due to interferences between beams transmitted and partially reflected at the silica–air and silica–glass interfaces. The deposition of an increasing number of layers of 590-nm particles on the top of the $(385 \text{ nm})_5$ stack first induces the appearance of a band around 1300 nm, which corresponds to the first-order Bragg peak of a 590-nm colloid lattice. Its intensity increases continuously with the number of 590-nm particle layers and its position shifts toward small wavelengths with the increasing number of layers of 590-nm beads. Such behavior was

observed by Galisteo–Lopez et al. for materials made of one size of colloids.¹⁸ Also, the intensity and the width of the peak around 830 nm increase with the successive depositions of 590-nm particles. This is due to the overlapping of this band with the secondary diffraction peak of the $(590 \text{ nm})_{1-6}$ stack (around 725 nm). This feature, previously mentioned by Colvin et al.,¹⁴ can be a powerful way to create photonic crystals with a broad stop-band. Fabry–Pérot fringes are also present at wavelengths above 1500 nm in all the NIR transmission spectra of the $(385 \text{ nm})_5/(590 \text{ nm})_{1-6}$ crystals. Indexing their positions allows us to estimate the thickness of the composite materials (for more details of the procedure, see ref 10). The plot of the global thickness (θ) as a function of the number of layers of 590-nm particles (N_{590}) exhibits a linear behavior (see inset of Figure 2). The slope of the straight line is equal to 500 nm, which is in good agreement with the thickness of one layer of 590-nm particles in an fcc structure, that is, $\sqrt{2/3} \times 590 = 482 \text{ nm}$. This result provides additional evidence of the good crystalline quality of the multilayer systems. Moreover, by assuming that θ is the sum of the thickness of the two fcc component stacks, that is, $\theta = \theta_{(385\text{nm})_5} + \theta_{(590\text{nm})_{N_{590}}} = (1 + 4\sqrt{2/3})385 + (1 + (N_{590} - 1)\sqrt{2/3})590$, one can deduce the thickness of the bottom stack made of five layers of 385-nm particles, $\theta_{(385\text{nm})_5}$, from the extrapolation of the linear curve to the y axis. We then find a value of $\theta_{(385\text{nm})_5}$ equal to $1.68 \mu\text{m}$, which is close to the predicted one, that is, $1.64 \mu\text{m}$.

Our capability to build multilayer colloidal crystals in a controlled manner was further exploited to study the influence of their architecture on their optical properties. Different $(385 \text{ nm})_j/(590 \text{ nm})_i$ and $(590 \text{ nm})_j/(385 \text{ nm})_i$ crystals having all a similar thickness (ca. $3.99 \pm 0.02 \mu\text{m}$) were elaborated. SEM side views of some of these composite materials ($i = 3/j = 6$; $i = 6/j = 4$; $i = 9/j = 2$) are presented in Figure 3. Once more, the good crystalline quality of the crystals and the smoothness of their top surface can be seen, even when the small particles are deposited onto the layers of large ones (Figure 4). This result, which is agreement with those previously reported,^{14,15} is indeed somewhat surprising as one can argue that the small spheres can be trapped in the interstitial spaces formed by the hexagonal close-packing of the large particles.

Figure 5A and 5B shows the NIR transmission spectra of the $(385 \text{ nm})_j/(590 \text{ nm})_i$ and $(590 \text{ nm})_j/(385 \text{ nm})_i$ composite materials, respectively. First, the incidence side of the light has no influence on the recorded spectra. All spectra exhibit Fabry–Pérot fringes at the same wavelengths, confirming that all the multilayer colloidal crystals have the same thickness. One can also see that the intensity of the Bragg peak around 1300 nm increases with the thickness of the stack made of larger spheres, while the position and the shape of the band around 800 nm are clearly related to the relative thickness of the component stacks. Either the Bragg peak of the crystal of 385-nm particles (when $\theta_{(385\text{nm})_i} > \theta_{(590\text{nm})_j}$) or the secondary diffraction peak of the crystal of larger spheres

(18) Galisteo-Lopez, J. F.; Palacios-Lidon, E.; Castillo-Martínez, E.; Lopez, C. *Phys. Rev. B* **2003**, *68*, 115109.

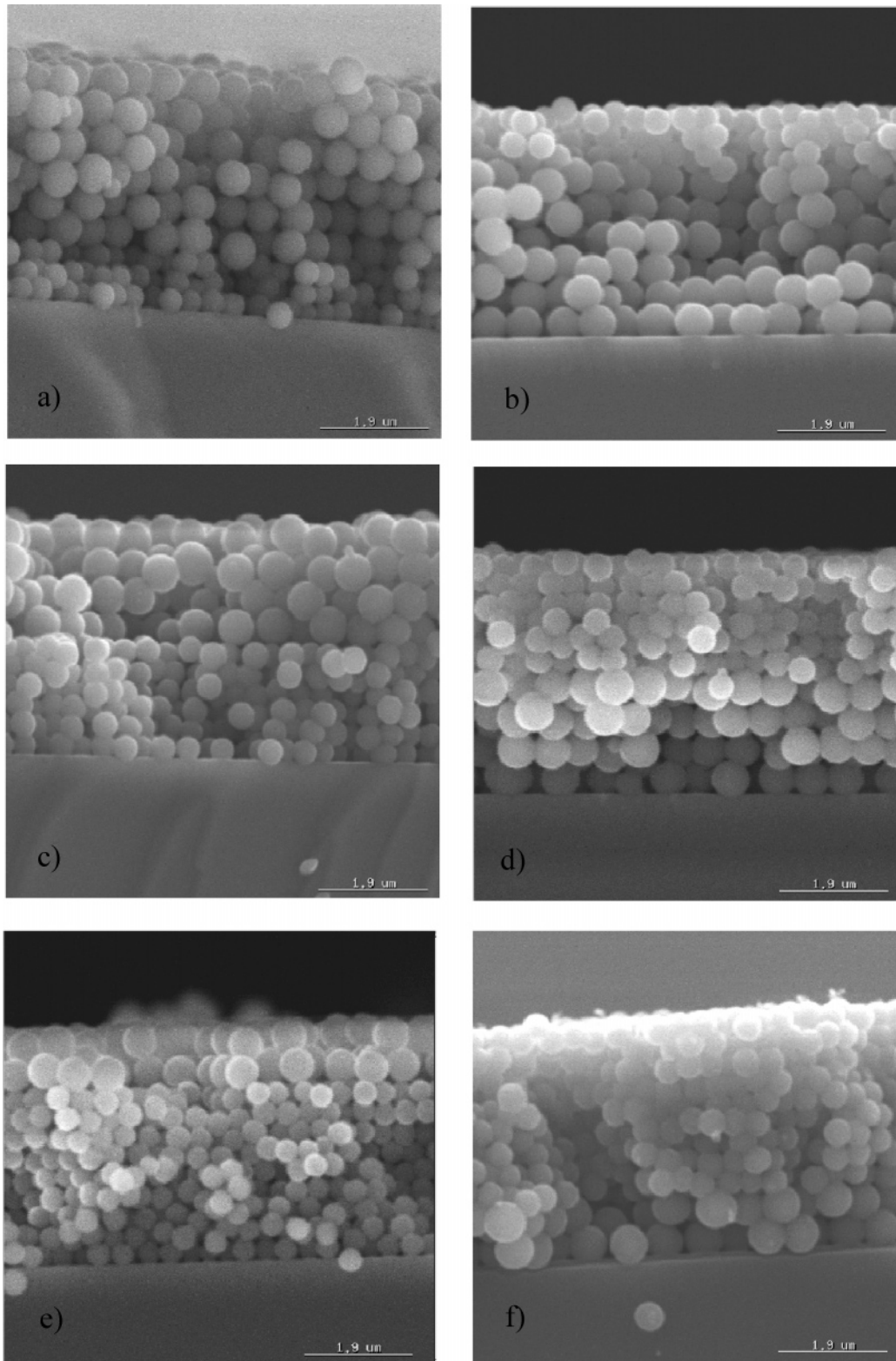


Figure 3. SEM side views of (a) $(385 \text{ nm})_3/(590 \text{ nm})_6$; (b) $(590 \text{ nm})_6/(385 \text{ nm})_3$; (c) $(385 \text{ nm})_6/(590 \text{ nm})_4$; (d) $(590 \text{ nm})_4/(385 \text{ nm})_6$; (e) $(385 \text{ nm})_9/(590 \text{ nm})_2$; and (f) $(590 \text{ nm})_2/(385 \text{ nm})_9$ colloidal crystals.

(when $\theta_{(385\text{nm})_i} < \theta_{(590\text{nm})_j}$) is prevailing, while the other one subsists as a small shoulder. In the intermediate case (when $\theta_{(385\text{nm})_i} \approx \theta_{(590\text{nm})_j}$), a unique broad and more or less resolved band can be seen. A closer comparison of the spectra displayed in Figure 5A and 5B allows one to state that the ordering of the stacking of the component crystals with one size of colloids has an influence of the optical properties of

the resulting composite crystals. For instance, periodic oscillations of the absorbance of the $(590 \text{ nm})_j/(385 \text{ nm})_i$ crystals in the 900–1150 nm range (indicated by the arrows in Figure 5B) cannot be seen in the spectra of the $(385 \text{ nm})_i/(590 \text{ nm})_j$ ones. This can be better seen in Figure 6, in which the spectra of the multilayer colloidal crystals are arranged in pairs. In a general manner, we can say that the spectra of

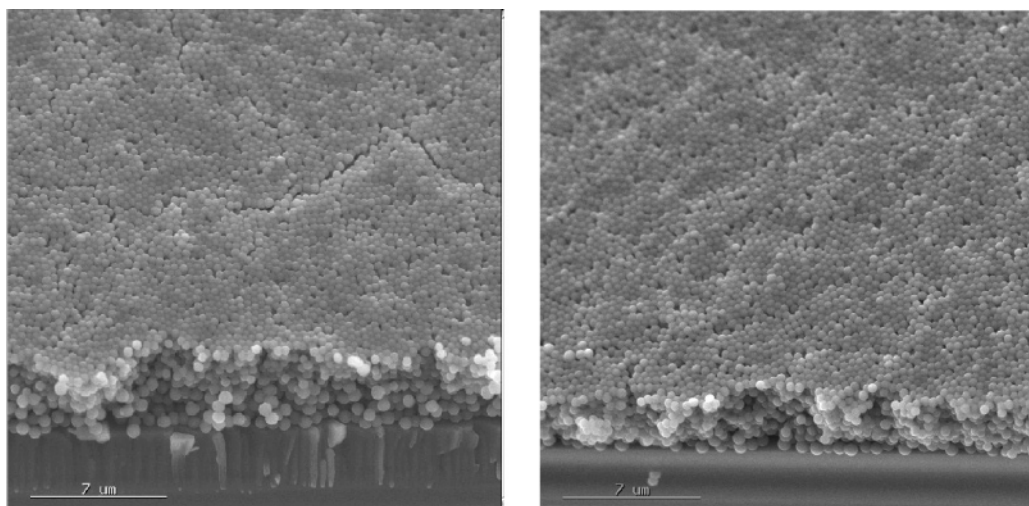


Figure 4. SEM top views of $(590 \text{ nm})_4/(385 \text{ nm})_6$ (left) and $(590 \text{ nm})_2/(385 \text{ nm})_9$ (right) colloidal crystals.

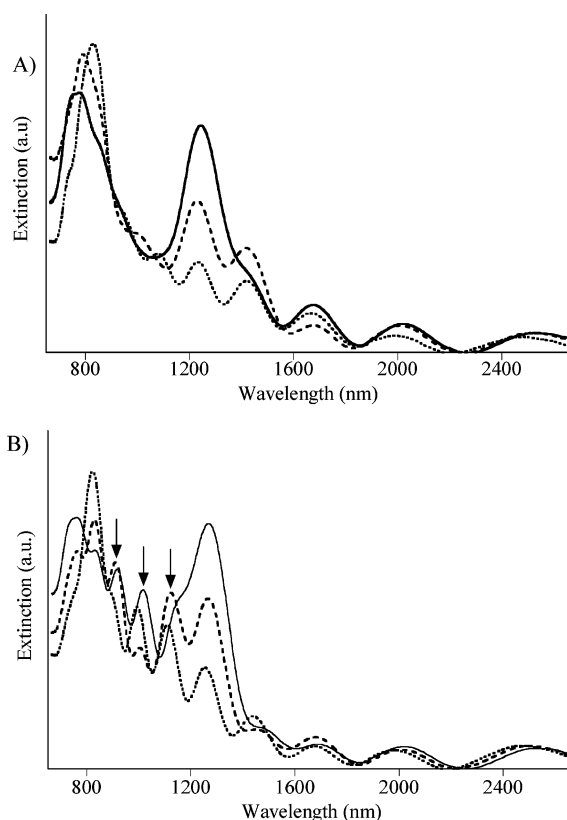


Figure 5. NIR transmission spectra of (A) $(385 \text{ nm})_9/(590 \text{ nm})_2$ (dotted line), $(385 \text{ nm})_6/(590 \text{ nm})_4$ (dashed line), $(385 \text{ nm})_3/(590 \text{ nm})_6$ (continuous line) colloidal crystals; (B) $(590 \text{ nm})_2/(385 \text{ nm})_9$ (dotted line), $(590 \text{ nm})_4/(385 \text{ nm})_6$ (dashed line), $(590 \text{ nm})_6/(385 \text{ nm})_3$ (continuous line) colloidal crystals.

the $(590 \text{ nm})_j/(385 \text{ nm})_i$ crystals are better resolved (particularly in the 700–1150 nm range), as they exhibit more peaks than those of the corresponding $(385 \text{ nm})_i/(590 \text{ nm})_j$ opals. This result, which is inconsistent with those reported by Colvin et al. a few years ago,¹⁴ can be partially explained by taking into account that $(590 \text{ nm})_j/(385 \text{ nm})_i$ crystals have an outside layer with a lower refractive index than the one of their inside layer, while the $(385 \text{ nm})_i/(590 \text{ nm})_j$ systems correspond to the opposite case. We are currently trying to model the optical properties of such composite materials to better understand their dependence on the ordering of the stacking of the component crystals.

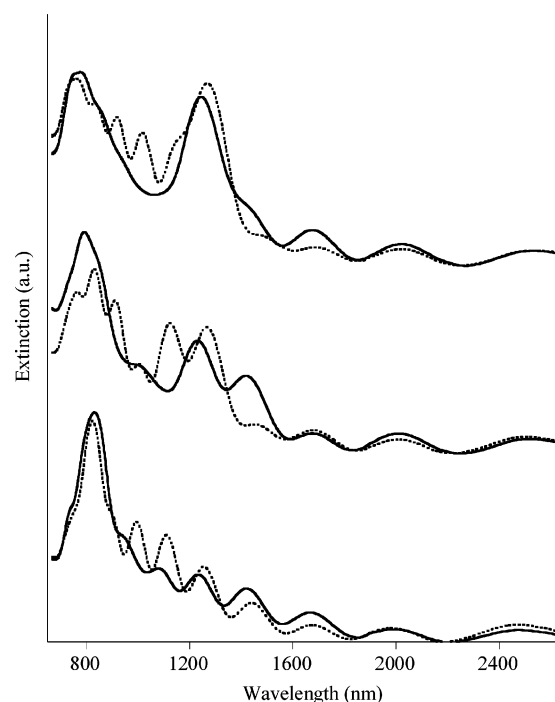


Figure 6. NIR transmission spectra of $(385 \text{ nm})_j/(590 \text{ nm})_i$ (continuous line) and $(590 \text{ nm})_i/(385 \text{ nm})_j$ (dotted line) colloidal crystals: $i = 3$ and $j = 6$ (top); $i = 6$ and $j = 4$ (middle); $i = 9$ and $j = 2$ (bottom). For better clarity, curves were shifted vertically.

By alternating deposition of 590- and 385-nm silica particles, we have also fabricated $((385 \text{ nm})_1/(590 \text{ nm})_1)_n$ and $((590 \text{ nm})_1/(385 \text{ nm})_1)_n$ colloidal crystals. Figure 7 shows SEM side views of the cases corresponding to $n = 3$. Despite the complexity of their architecture, these materials exhibit a uniform ordering over large areas. They can then be assimilated to one-dimensional photonic crystals with three-dimensional substructure, which may find potential applications in interference coating.¹⁹ The NIR transmission spectra of these systems (see Figure 8) exhibit five main bands around 750, 940, 1160, 1510, and 2250 nm. Once again, the stacking order has a strong influence on the optical properties of the heterostructures.

(19) Southwell, W. H. *Appl. Opt.* **1997**, *36*, 314.

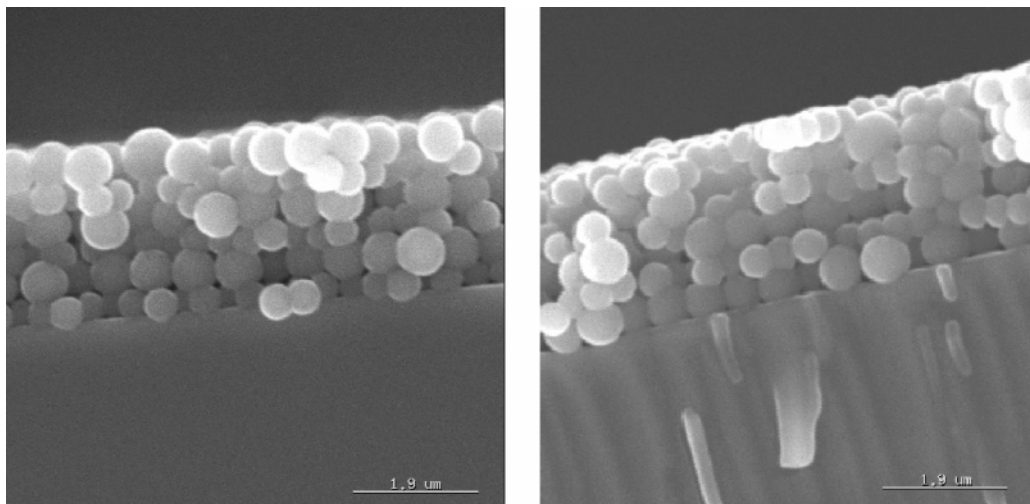


Figure 7. SEM side views of $((385 \text{ nm})_1/(590 \text{ nm})_1)_3$ (left) and $((590 \text{ nm})_1/(385 \text{ nm})_1)_3$ (right) colloidal crystals.

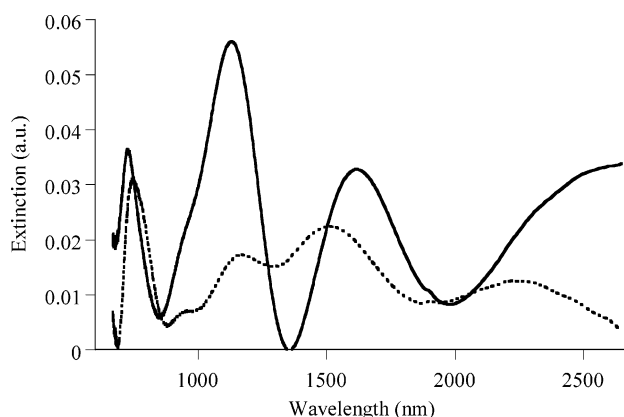


Figure 8. NIR transmission spectra of $((590 \text{ nm})_1/(385 \text{ nm})_1)_3$ (continuous line) and $((385 \text{ nm})_1/(590 \text{ nm})_1)_3$ (dotted line) colloidal crystals.

Conclusion

In summary, we have successfully engineered multilayer colloidal crystals in which each stack has a thickness controlled at the layer level using the Langmuir–Blodgett technique. By increasing the number of layers of large spheres deposited on the top of a stack of small ones, we

have shown that the optical properties of the composite materials can be tailored with a great accuracy. We have also demonstrated that colloidal crystals with a similar global thickness and an inverse stacking ordering do not have the same optical behavior. A “superlattice” colloidal crystal consisting of alternating layers of two different sphere sizes has been built. We do believe that these few examples of multilayer colloidal crystals are the first step toward the fabrication of more sophisticated systems with specific and in-situ tunable optical properties. Experiments to reach these goals are currently under progress in our laboratory. The fabrication of multilayer crystals consisting of stacks of microgels or magnetic colloids with optical properties which can be tuned in response to the environmental changes will be reported soon.

Acknowledgment. We thank S. Reculosa, F. Guillaume, and T. Buffeteau for fruitful discussions and B. Agricole and E. Sellier for Langmuir–Blodgett and SEM experiments, respectively.

CM050601V